



# Optimized conditions for cobalt diffusion in Sri Lankan colorless topaz and coloration mechanism elucidation through spectro-chemical investigation

Chandana. P. UDAWATTE<sup>1</sup>, Sunil ABEYWEERA<sup>3</sup>, L. R. K. PERERA<sup>3</sup>, Sandun ILLANGASINGHE<sup>4,\*</sup>, Chirath WEERASOORIYA<sup>1</sup>, Chakkaphan SUTTHIRAT<sup>5</sup>, Naleen JAYASINGHE<sup>4</sup>, Tilak DHARMARATNE<sup>4</sup>, and Saranga DIYABALANAGE<sup>6,7</sup>

<sup>1</sup>Department of Physical Science and Technology, Faculty of Applied Sciences, Sabaragamuwa University of Sri Lanka, Belihuloya, 70140, Sri Lanka.

<sup>2</sup>Ameran Gems Pvt Ltd, Arunachalum Avenue, Horton Place, Colombo 7, Sri Lanka

<sup>3</sup>Department of Geology, Faculty of Science, University of Peradeniya, Peradeniya, 20400, Sri Lanka.

<sup>4</sup>Gem and Jewellery Research and Training Institute, Regional Centre, Hidellana, Ratnapura, 70012, Sri Lanka.

<sup>5</sup>Department of Geology, Faculty of Science, Chulalongkorn University, Bangkok, 10330, Thailand.

<sup>6</sup>Instrument Center, Faculty of Applied Sciences, University of Sri Jayewardenepura, Gangodawila, Nugegoda, 10250, Sri Lanka.

<sup>7</sup>Ecosphere Resilience Research Centre, Faculty of Applied Sciences, University of Sri Jayewardenepura, Nugegoda, 10250, Sri Lanka.

\*Corresponding author e-mail: sillangasinghe@gmail.com

## Received date:

14 November 2022

## Revised date

5 January 2023

## Accepted date:

9 January 2023

## Keywords:

Co diffusion;

Blue topaz;

Heat treatment;

Coloration of blue topaz

## Abstract

Most of natural topaz is colorless; thus, methods of color enhancement are widely used for coloring this mineral. Currently, blue color is obtained by cobalt diffusion due to drawbacks in existing coloration methods. In this study, optimum conditions suitable for Cobalt diffusion in Sri Lankan colorless topaz were investigated and coloration mechanism was elucidated. The diffusion agent was prepared by mixing  $\text{CoCO}_3$  with  $\text{Na}_2\text{CO}_3$ ,  $\text{CaCO}_3$  and carbon powder and diffusion was carried-out by varying the temperature and soaking time. Chemical analysis, UV-Vis absorption spectrum, infrared absorption spectra, and Raman peaks of diffused and non-diffused topaz were tested. The results clearly indicated that the optimum condition for Co diffusion in Sri Lankan topaz is  $950^\circ\text{C}$  for 11 h. The EPMA analysis showed that the Co concentration in the diffused sample varied from 0.001 wt% to 0.027 wt% while colorless topaz showed  $<0.001$  wt%. The UV-Vis spectrum of Co diffused blue topaz gave three absorption peaks at 556, 588, and 627 nm corresponding to three spin-allowed electronic transitions of  $\text{Co}^{2+}$  ion in tetrahedral coordination. In case of Co diffused topaz, one additional new broader IR absorption peak was noticed around  $6640\text{ cm}^{-1}$  presumably arising by optical transitions of  ${}^4\text{A}_2 \rightarrow {}^4\text{T}_1$  in  $\text{Co}^{2+}$  ( ${}^4\text{F}$ ). Our results lead to the conclusion that, blue color of the Co diffused topaz is arising by spin-allowed electronic transitions of  $\text{Co}^{2+}$  ions in tetrahedral site of topaz matrix through substitution of  $\text{Si}^{4+}$  ions.

## 1. Introduction

Topaz is an aluminum fluorosilicate mineral with the chemical formula of  $\text{Al}_2\text{SiO}_4(\text{F}, \text{OH})_2$ . Major chemical variation of different types of topaz is determined by the  $[\text{OH}]/[\text{F}]$  concentration ratio. Topaz consists of  $\text{Al}[\text{O}_4(\text{F}, \text{OH})_2]$  octahedral chains which are linked to isolated tetrahedral  $\text{SiO}_4$  units. Generally, topaz crystallizes in the orthorhombic system but the extent of OH/F substitution turns its symmetry into triclinic and occurs as an accessory mineral in aluminous rocks [1].

Topaz is often colorless, but it occurs naturally in a variety of colors such as pale blue, yellow, brown, orange, and pink, etc. [2]. The occurrences of these colors are mainly determined by the presence of lattice defects known as color centers [3]. Defects consist of missing or misplaced atoms or electrons. These defects may have originated at the time of mineral formation or may have been introduced later

by external influences such as fast neutron irradiation [4]. Additionally, these colors are also affected by the presence and variations in the amounts of F, OH, and minor impurities in the material. Crystals with more OH are yellow to brown in color, while those with more F are typically blue or colorless. Pink-red and violet stones contain chromium as an impurity in the crystal structure [2]. However, most of the natural topaz is colorless; thus, color enhancement methods are widely used to convert these stones to beautiful gemstones.

Different coloration methods such as irradiation followed by heating, surface coating, surface modification, and surface diffusion have been introduced to give color to colorless topaz [5-7]. Among them, irradiation is the most common method used to obtain blue topaz where color centers are produced by exposing topaz either to gamma rays or neutrons or electrons, followed by low-temperature heating [8-11]. Though the method is effective, the main limitation is the radioactivity induced by irradiation [4,12]. Neutron irradiated

blue topaz has to be kept aside for several months, until its residual radioactivity reaches a safer level of less than 74 Bq/g or 2 nCi/g, as defined by the Nuclear Regulatory Commission (NRC) [12]. Sometimes, it may have to be kept away for more than one year. Such long delays cause a loss of revenue to the manufacturer; thus, premature radioactive colored topaz is released into the market [13]. In addition to that, the irradiation methods have significant drawbacks in terms of cost, safety, and efficacy. Further, in some developing countries such as Sri Lanka where the colorless topaz is abundant [4], facilities are inadequate to use irradiation as a value addition method.

Therefore, currently, the blue color is obtained by diffusion of cobalt ( $\text{Co}^{2+}$ ) ion by heating cobalt coated colorless topaz at 1024°C for 24 h [6]. However, subjecting the mineral to high temperatures for a prolonged period can create external and internal damages in the structure of the material. Crystallographic, optical, and chemical properties of topaz can vary with chemical composition, which reflects the petro-genesis of the rocks in which the individual crystal formed [14]. Therefore, optimum cobalt diffusion conditions perhaps may slightly deviate with the petro-genesis or locality. Hence, the identification of an optimum cobalt diffusion condition at low temperatures with short soaking time is imperative, as well as time and cost effective. Although it required detailed investigations on chemical and spectroscopical characteristics of Co diffused topaz, such studies are limited and the color formation process of Co diffused topaz is hitherto unknown.

Sri Lanka is an island which is well known for its fine gemstones. Most of the gem-quality material is found in alluvial deposits throughout the island. Among them, the largest untreated and treatable gem material is colorless topaz (Figure 1) [15]. However, no coloration process is undertaken to enhance the value of this colorless topaz. Therefore, introducing an easy, non-harmful and economically viable method for coloring colorless topaz is essential to the trade.

Moreover, the coloration mechanism of Cobalt diffusion blue topaz is still hitherto unknown. Therefore, elucidating of coloration mechanism of Cobalt diffused blue topaz is paramount important to the scientific community. In this study, a modified treatment method was tested followed by chemical and spectroscopic analysis with the intension of introducing optimum conditions for Co diffusion in Sri Lankan topaz. The changes in physical and chemical properties after diffusion were investigated by EPMA, EDXRF, UV-VIS, Raman, and FTIR spectroscopic analysis. Subsequently, based on the characterization results, the cause of color change in cobalt diffused topaz was elucidated for the first time.

## 2. Materials and methodology

### 2.1 Sample collection, preparation, and gemological properties

Rough colorless topaz samples (Figure 2) were collected from Ratnapura gem market which is one of the world's reputed gem markets located in Sri Lanka. Initially, the collected stones were immersed in bromoform to distinguish topaz from quartz. Selected topaz samples were further examined with the microscope (KRÜSS OPTRONIC, Germany) and samples with fewer defects were chosen for the treatment. The weight of each sample was measured with a carat

weighing scale (Vibra CT, Japan). Refractive indices and luminescence characteristics of the samples were examined by using a refractometer (Fable FB/R02, China) and UV lamp (Module 6-System Eickhorst, Germany). The internal features such as color diffusions, inclusions, cracks, and fractures, etc., were examined with a horizontal stage microscope. Optical absorption spectrum of the samples were obtained using OPL spectroscopy. Before subjected to the treatments, each sample was cut into slices of ~ 3 mm thickness, polished and separated into three groups.

### 2.2 Preparation of diffusion material and heating process

The diffusion material used in the study was prepared with analytical grade  $\text{CoCO}_3$ ,  $\text{Na}_2\text{CO}_3$ ,  $\text{CaCO}_3$ , and carbon powder collected from a kerosene oil lamp (buckyball). The components of  $\text{CoCO}_3$ ,  $\text{Na}_2\text{CO}_3$ , and  $\text{CaCO}_3$  were mixed in the ratio of 1:1:1 to form a slurry. The Co content of the slurry was approximately 15% by weight. In this composition, carbon powder was used as a base material with  $\text{CoCO}_3$ . In previous studies,  $\text{Co}^{2+}$  ion in the form of  $\text{CoO}$  has been used as the coloring material [5,6] whereas  $\text{CoCO}_3$  was used in the current study. Out of the three sample groups, two groups were rolled in the prepared slurry to get an evenly coated chemical layer (<0.5 mm) all around the stones and were allowed to dry for 4 h. The remained group of samples was used as the controls.

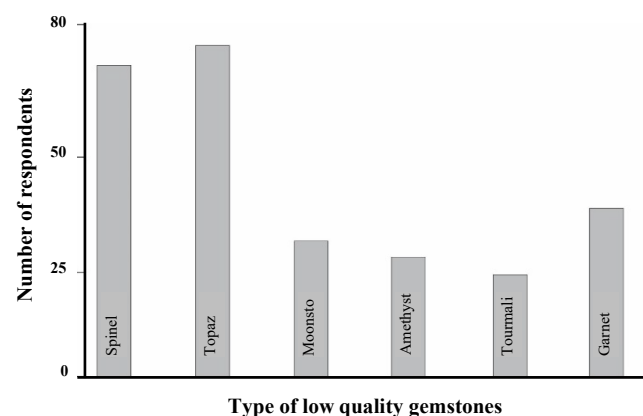


Figure 1. Availability of low gem quality materials in Rathnapura gem trade (after Illangasinghe *et al.*, 2019).

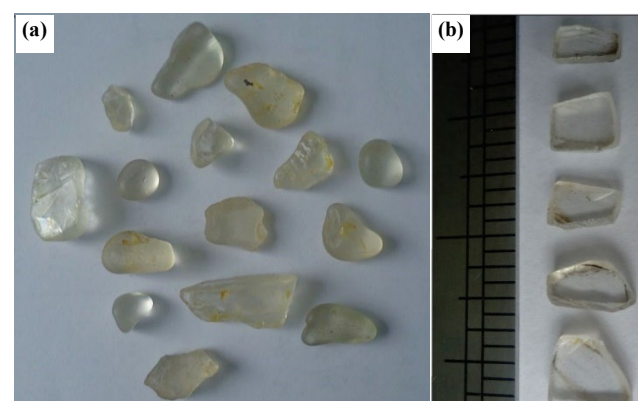


Figure 2. Colourless topaz samples available in Sri Lankan gem trade; (a) rough colourless topaz samples, (b) sliced and polished samples prepared for cobalt diffusion.

Heat treatment was carried out using muffle furnace (Carbolite CWF 11/13). Different batch experiments were performed by varying the temperature and soaking time. After coated with prepared slurry, three batch experiments were performed at temperatures of 900°C, 950°C and 1000°C for 11, 15, 20, and 25 h accordingly under oxidizing condition. To study the effect of temperature on cobalt diffusion, previously treated first batch was re-heated at 950°C. Moreover, resulted samples of the second batch treatment were re-heated under the same condition for three times. Finally, fourth batch of samples that were dip in a dry mixture of carbon powder and  $\text{CoCO}_3$  were subjected to heat treatment at 950°C for 25 h. All resulted colors were clearly examined and further chemical and spectroscopical analysis were performed only for the gem quality Co diffused blue topaz and untreated colorless topaz.

### 2.3 Chemical analysis

Measuring the cobalt concentration of the diffused and reference colorless samples is more imperative to acquire an idea on cobalt diffusion. Quantitative CoO and other major element contents across the surface of the diffused and non-diffused samples were analyzed using a JEOL Electron Probe Micro-Analyzer (EPMA) (JXA-8100, Japan). Pure oxide and mineral standards were used as standards for calibration. Analyses were performed at 15 kV (accelerating voltage), with a beam current of 24 nA and focused beam with a probe diameter smaller than 1  $\mu\text{m}$ . Measuring times were set to 30 s and 10 s for peak counts and background counts, respectively. Ten (10) points across the diffused and reference samples were tested.

### 2.4 Spectroscopic analysis

To determine the effect of chromophores on cobalt ion in colored topaz, UV-VIS absorption spectra were obtained using UV-Visible Spectrometer (Shimadzu UN-160, Japan and GemmoSphere™ UV-Vis-NIR spectrometer, Finland).

The infrared (IR) absorption spectrum of a mineral gives information on the bond structure. The vibration frequency of chemical bonds corresponds to the lattice ordering and bond length of the topaz structure. These bond characteristics were studied using Fourier Transform Infrared (FTIR) and Raman spectroscopy. The infrared absorption spectrum of topaz is a reliable analytical method to find out the occurrence of hydroxyl groups and the presence of impurity elements in topaz [16]. Infrared absorption spectra of Co diffused and colorless topaz was examined using an FTIR Spectrophotometer (GemmoFtir™, Finland). Un-polarized IR absorption spectra were recorded from  $\sim 400\text{ cm}^{-1}$  to  $7000\text{ cm}^{-1}$  with  $4\text{ cm}^{-1}$  resolutions and the range from  $1000\text{ cm}^{-1}$  to  $7000\text{ cm}^{-1}$  was used in the interpretations.

To study the structure of the mineral, Raman spectra of cobalt diffused and colorless topaz was obtained using a Raman spectrometer (GemmoRaman-532™, Finland). Absorption spectra were recorded from  $225\text{ cm}^{-1}$  to  $4700\text{ cm}^{-1}$  with  $11\text{ cm}^{-1}$  resolution.

## 3. Results and discussion

### 3.1 Classical gemological properties of Co diffused and colorless topaz

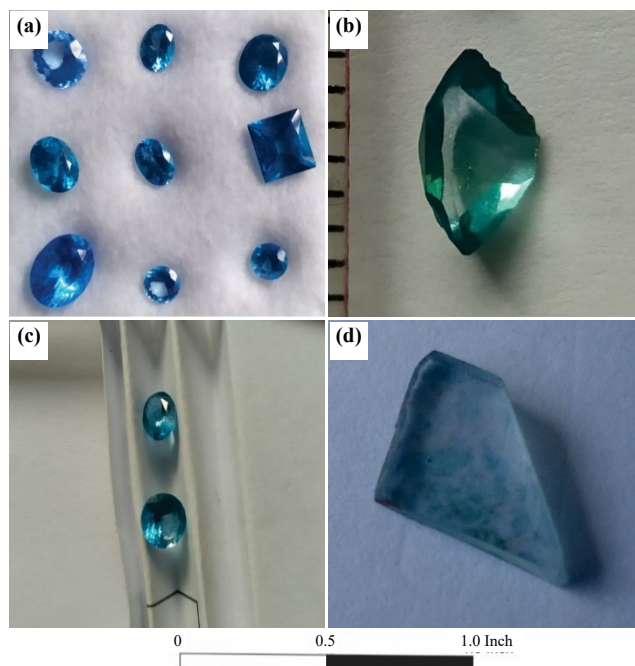


**Figure 3.** Cobalt diffused blue topaz with different treatment conditions. (a) Co diffused at 950°C for 11 h, (b), Co diffused at 900°C, (c) Co diffused green topaz re-heated at 950°C for 11 h and (d) dry powder diffused topaz at 950°C.

All the topaz specimens selected for this study were colorless and free from inclusions. The weight of selected specimens ranged from 0.53 carats to 4.17 carats. They showed a refractive index (RI) in the range of 1.610-1.620 and their birefringence was 0.010.

However, anomalous RI values greater than 1.81 observed for the Co diffused topaz (Figure 3). Based on X-Ray Photoelectron Spectroscopy (XPS) analysis, it has been revealed an enrichment of Si in the outermost layer of the Co diffused topaz while the concentrations of Al and Co were considerably depleted [5]. However, at depths between 10 nm to 50 nm, Si concentration become depleted to below detection limits, while Al and Co concentration reached their maximum. Previous studies have reported a decomposition of the outermost layer under elevated temperature conditions where topaz surface decomposed to mullite and other silicate phases [17-19]. However, the decomposition of the outermost layer of Co diffused topaz is not yet well known. The layer between 10 nm to 50 nm is enriched with Al and forms a Co-aluminum complex which has been identified as a spinal phase [5]. In this phase, Si ions are perhaps replaced by the Co ions in the topaz matrix; consequently, these released Si ions may be involved in the formation of Si enriched outermost layer. As such, Co diffusion performed at 950°C for 11 h in the present study may have caused a phase change in the outer surface layer resulting a high RI value.

In both untreated and treated samples, no any clear distinguishable absorption bands in visible spectrum were observed under the classical gemological spectroscopy. Untreated samples didn't show any fluorescence effect in the short or long wave ultra violet condition while the treated sample was given a chalky glow. Moreover, untreated sample was seen in black after examined through Chelsea color filter while red was given for the treated samples. Therefore, ultraviolet lamp and Chelsea color filter can be used to distinguish cobalt diffused topaz.

The color of the treated colorless topaz varied from bluish-green to greenish-blue color (Figure 3). Microscopic observations showed a spotty coloration in diffused samples where the observation is comparatively higher in the samples diffused by the dry powder method. Colorless topaz became green in color when diffusion was performed at 900°C for 11, 15, 20, and 25 h (Figure 3(b)). This green color formed by Co diffusion has been identified as unstable position in the topaz lattice compared to the blue color [20]. It was identified that an intense blue coloration in topaz can be obtained when the diffusion is carried-out at 950°C for 11, 15, 20, and 25 h (Figure 3(a)), however, gem quality blue color topaz was resulted by heating at 950°C for 11 h. Moreover, no any external damage or spotty coloration was observed in this gem quality blue topaz under the naked eye. Further, the aforementioned green color also can be turned into a blue color by re-treating them at 950°C for 11 h (Figure 3(c)). However, the presence of spotty coloration can be observed in the dry powder diffusion process, even with the naked eye (Figure 3(d)). In contrast, melted surfaces were observed after heating at 1000°C for 11, 15, 20, and 25 h which implies the unsuitability of higher temperatures in Co diffusion treatments for Sri Lankan topaz. Therefore, it could be suggested that the optimum Co diffusion treatment conditions for colorless topaz found in Sri Lanka are 950°C for 11 h.

### 3.2 EPMA analysis

Average content of Al<sub>2</sub>O<sub>3</sub>, SiO<sub>2</sub>, F, CaO, FeO, MgO, and CoO in the colorless topaz were reported as 51.838±0.334, 32.940±0.15, 14.736±0.212, 0.022±0.014, 0.011±0.008, 0.012±0.008 and <0.001 wt% accordingly. However, the same in the Co diffused samples were reported as 51.677±0.435, 33.153±0.216, 14.671±0.277, 0.0118±0.007, 0.013±0.007, 0.0078±0.008, 0.0172±0.011 wt%. Among the analyzed elements, Al<sub>2</sub>O<sub>3</sub>, SiO<sub>2</sub>, and F show chemical homogeneity and FeO

and MgO did not show chemical homogeneity across the sample (Table 1).

Comparatively high F content is typically recorded in topaz from pegmatites and is ~19.5 wt% [21]. However, the studied topaz indicated F contents around 14.7 wt% which is lower than the above value. However, similar F contents were recorded in imperial topaz from Brazil originated by metamorphic tectono-thermal events [22]. Moreover, cobalt diffused blue topaz showed that the CoO content varied from <LOD to 0.027 wt% which confirms the cobalt diffusion into the topaz matrix. The chemical analysis revealed that the Co ion concentrations across the diffused samples are uneven and suggest a spotty surface coloration under the microscopical scale. However, the influence of temperature and soaking time on Co diffused depth variation was not addressed in this current study and needs further investigation.

### 3.3 Results of UV-visible spectroscopic analysis

The UV-Visible spectra of colorless and cobalt diffused blue topaz are shown in Figure 4. In both Co treated and untreated samples, an absorption peak was observed at ~420 nm and the edge of this asymmetric broad peak extended to 680 nm. This peak has been assigned to O<sup>2-</sup> center interaction with Al ions or due to presence of impurities of Cr, Fe and Mn [23]. The peak was remained after heating up to 950°C, thus implies its thermal stability.

No any additional peaks were observed in colorless topaz (Figure 4). Therefore, the resulted UV-visible absorption spectrum for colorless topaz imply the absent of any color forming element in the topaz matrix in detectable levels. Interestingly, Cobalt diffused blue topaz showed a new broad intense absorption peak between 520 nm and 720 nm, correspond to the resulted blue colour. This broad peak is composed of several narrowed peaks at about ~550, ~588, and ~625 nm.

**Table 1.** Major chemical composition of Co diffused blue topaz and colourless topaz, Sri Lanka (unit; wt%).

Point number	F	Al <sub>2</sub> O <sub>3</sub>	CaO	FeO	SiO <sub>2</sub>	MgO	CoO	Sample
12	15.128	51.665	0.014	0.003	33.455	0.002	0.004	Co diffused blue topaz sample
13	14.864	51.643	0.011	<0.001	32.683	0.002	<0.001	
14	14.847	51.478	0.007	<0.001	33.253	<0.001	<0.001	
15	14.552	51.235	0.003	<0.001	33.358	<0.001	<0.001	
16	14.725	51.942	0.016	<0.001	33.045	<0.001	0.018	
17	14.436	51.306	<0.001	0.024	33.177	0.025	<0.001	
18	14.722	51.404	0.003	<0.001	33.089	0.007	0.017	
19	14.567	52.172	0.015	<0.001	33.259	<0.001	0.027	
20	14.105	52.587	0.017	<0.001	32.998	0.003	0.01	
21	14.768	51.335	0.021	<0.001	33.217	<0.001	0.027	
22	15.233	51.203	<0.001	0.018	33.151	<0.001	<0.001	
23	14.694	51.489	0.042	0.012	32.938	0.011	<0.001	
24	14.717	51.477	0.032	<0.001	33.171	0.014	<0.001	
25	14.819	52.165	0.018	0.007	32.883	<0.001	<0.001	
26	14.656	51.842	0.006	0.002	33.007	0.005	<0.001	
27	14.771	51.989	0.012	0.025	32.917	0.026	<0.001	
28	14.407	52.177	<0.001	<0.001	32.856	0.004	<0.001	
29	14.81	52.052	<0.001	0.009	32.998	<0.001	<0.001	
30	14.689	51.911	<0.001	0.005	32.788	<0.001	<0.001	
31	14.571	52.08	<0.001	<0.001	32.692	<0.001	<0.001	

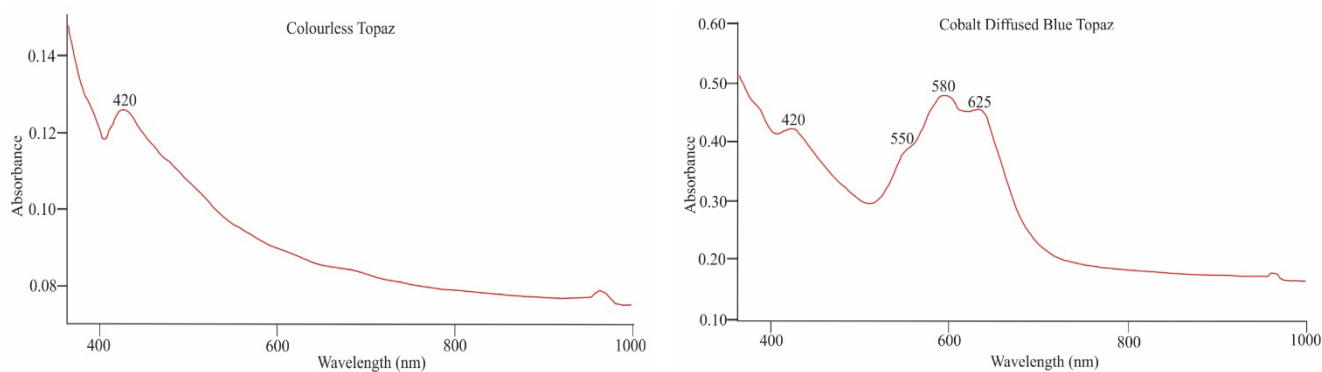


**Figure 4.** UV-Visible absorption spectrum of colorless topaz and cobalt diffused blue topaz.

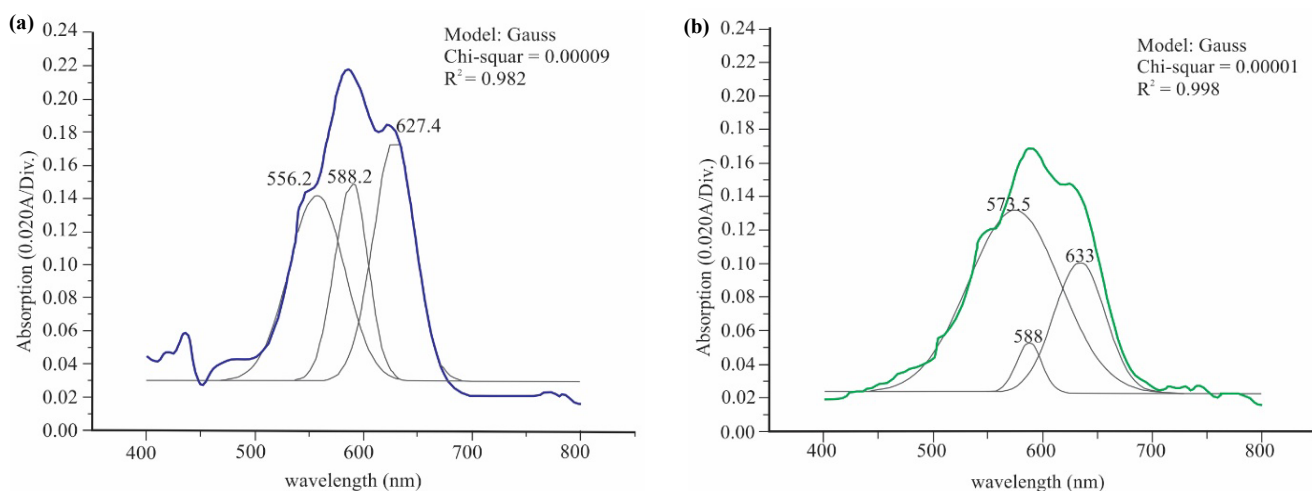


**Figure 5.** UV-Visible absorption spectra with Gaussian curve fitting: (a) blue and (b) greenish blue color topaz obtained after Co diffusion.

Figure 5 depicts the UV-Visible absorption spectra of resulted blue and greenish blue color topaz with Gaussian curve fitting. The  $R^2$  and chi-squar values of curve fitting of blue topaz were 0.982 and 0.00009 respectively. In the spectrum of blue topaz, a broad triplet peak from  $\sim 450$  nm to 700 nm was observed. The Gaussian fitting showed that this broad peak is composed of three absorption peaks occurred at 556.2, 588.2, and 627.4 nm with absorption intensities of 0.14, 0.15, and 0.17 respectively (Figure 5). In topaz matrix, trace elements substitution is possible at two sites which are the  $\text{Si}^{4+}$  ion site in tetrahedral coordination and  $\text{Al}^{3+}$  ion site in octahedral coordination. Different trace elements can substitute in these two sites [22,24,25]. However, distinct minerals having  $\text{Co}^{2+}$  ions have given similar triplet absorption peaks and consequently those minerals have given a blue color [26-30]. The  $\text{Co}^{2+}$  ions in these minerals occupied the tetrahedral coordination as demonstrated by Co bearing natural blue quartz, Co-doped synthetic quartz [28], Co bearing spinel [27,31], Co bearing staurolite [29], Co-doped gahnite [32], Co-staurolite [33], and synthetic Co-doped Mg-spinel [30]. On the other hand, octahedrally coordinated  $\text{Co}^{2+}$  sites are not consistent with the observed optical spectrum [28]. Therefore, in the present study,  $\text{Co}^{2+}$  ions may have diffused into topaz matrix and presumably substituted for  $\text{Si}^{4+}$  ions in tetrahedral sites. This process can be verified by the chemical composition variation in Co diffused outer layer where Al was enriched while Si was depleted [5]. However, ionic charge and radius of  $\text{Co}^{2+}$  and  $\text{Si}^{4+}$  are different.

However, this different ionic charge may be charge compensating in tetrahedral site by monovalent ions. Likewise, lattice distortion may be occurred due to ionic radius differences. However, further investigations are required on this for detail explanation.

Further, the inference that  $\text{Co}^{2+}$  ions occupied the tetrahedral coordination of Co diffused blue topaz can be reasoned-out considering energies of spin electronic configurations. Octahedrally coordinated ion complexes have high spin electronic configurations. Based on the theory and following the Tanabe-Sugano diagram for tetrahedral  $\text{Co}^{2+}$ , during three spin-allowed electronic transitions, increasing transition energies are expected as:  ${}^4\text{A}_2 \rightarrow {}^4\text{T}_2(4\text{F})$ ,  ${}^4\text{A}_2 \rightarrow {}^4\text{T}_1(4\text{F})$  and  ${}^4\text{A}_2 \rightarrow {}^4\text{T}_1(4\text{P})$  [29,34]. Energy difference between the ground state and exiting state of these three spin-orbit transition matches with the three absorption peaks at 556.2, 588.2, and 627.4 nm observed in the present study. Therefore, red, yellow, and green parts of the visible light region were absorbed by  $\text{Co}^{2+}$  in tetrahedral site with spin-orbit transitions. Remaining transmitted region in visible light is responsible for the color of  $\text{Co}^{2+}$  diffused topaz. Consequently, blue color was given for Co diffused topaz in accordance with other blue color minerals mentioned above.

The Gaussian curve fitting of UV-Visible absorption spectrum of Co diffused green color topaz is shown in Figure 5(b). The  $R^2$  and chi-squar values of curve fitting correspond to green topaz were 0.998 and 0.00001 respectively. Integral absorption peaks were slightly

deviated with blue color absorption spectrum. The intensity of integral absorption peaks were lower than the corresponding peaks resulted for blue topaz. The absorption peak at 556.2 nm of blue topaz has slightly moved its peak position to 573.5 nm in green color topaz and has become broader. Nevertheless, other two peaks (588.2 nm and 627.4 nm) positions remained unchanged. However, comparatively low intensities were observed in peaks positioned at 573.5, 588, and 633 nm, where the intensities were 0.13, 0.04, and 0.10 respectively (Figure 5(b)). These slight deviations in UV-Visible absorption spectrum of green color topaz may have resulted from occupying unfavorable positions in the lattice by Co ions [20] at comparatively low temperature diffusion. Taran *et al.* (2009) [29] emphasized that coordination and symmetry play an important role in the intensity gaining mechanism of absorption peaks of  $\text{Co}^{2+}$ . Thus, coordination and symmetry around  $\text{Co}^{2+}$  ions in green topaz may differ from blue topaz and may have resulted in absorption intensity differences of the three distinct peaks considered.

### 3.4 Results of IR absorption spectra

IR absorption spectra of Co diffused and colourless topaz depicted five distinct IR absorption bands clustered around 1000-2050, 2300-3000, 3300-4100, 4200-4850, and 6000-7000  $\text{cm}^{-1}$  (Figure 6). IR absorption peaks observed in 1000-2050  $\text{cm}^{-1}$  region are attributed to stretching of Al-O bonds and Si-O bonds in the topaz matrix [16,35]. Similar bands were also observed by Smith (1995) [36] due to Al-O bonds in corundum.

Distinguished four IR absorption peaks were recorded in the region of 2300  $\text{cm}^{-1}$  to 3000  $\text{cm}^{-1}$  (Figure 6). Dominant sharp absorption peak appeared at 2312  $\text{cm}^{-1}$  while comparatively weak absorption peaks occur at 2600, 2760, and 2918  $\text{cm}^{-1}$ . Similar pattern in all peaks in that area were observed in different Co diffused and colorless samples in spite of their different heat treatments. Previous researchers have interpreted the particular peaks in this IR absorption region as stretching vibration of bonded OH molecule [23,37]. Furthermore, It has been experimentally revealed that the position of hydrogen in the structure of topaz-OH by means of ab-initio quantum techniques with IR absorption pattern [37]. Accordingly, this study has attributed the two peaks near 2300  $\text{cm}^{-1}$  to stretching of topaz-OD (Deuterium) [37]. Thus, sharp dominant peak at 2312  $\text{cm}^{-1}$  observed in the present study is most probably associated with topaz-OD stretching. Moreover, IR absorption peaks around 2300  $\text{cm}^{-1}$  to 2700  $\text{cm}^{-1}$  are accorded with stretching of Topaz-OD [38]. Therefore, minor absorption peak at 2700  $\text{cm}^{-1}$  is also attributed to stretching of Topaz-OD.

Five IR absorption peaks at 3351, 3453, 3640, 3828, and 3944  $\text{cm}^{-1}$  appeared in the 3300  $\text{cm}^{-1}$  to 4000  $\text{cm}^{-1}$  region. Absorption peaks in this region are mainly be attributed to various OH vibration modes [10,11,16,24,35,38-41]. Most prominent absorption peak in this region is at 3640  $\text{cm}^{-1}$ . This peak was appeared in both Co diffused and colorless topaz. The hydroxyl stretching vibration peak of topaz is commonly given at 3650  $\text{cm}^{-1}$  and this anticipated peak was not observed in the present study. Nevertheless, the IR peak at 3650  $\text{cm}^{-1}$  was decomposed in two components at 3639  $\text{cm}^{-1}$  and 3650  $\text{cm}^{-1}$  [16]. Moreover, these two peaks were assigned to two stretching modes of the OH molecules substituting F ions in topaz [42]. Thus, most prominent IR peak observed at 3640  $\text{cm}^{-1}$  in the present study may

assigned to stretching modes of the OH molecules substituting for F ions in topaz. Two minor peaks appeared at 3351  $\text{cm}^{-1}$  and 3453  $\text{cm}^{-1}$  (Figure 6) may attributed to the anomalous OH groups attached to lattice defects of topaz [11,16,37-39,41,43,44]. The remainder of the absorptions at 3828  $\text{cm}^{-1}$  and 3944  $\text{cm}^{-1}$  agree well with those reported in previous studies and were assigned to “mirror image” peaks at 3300  $\text{cm}^{-1}$  to 3500  $\text{cm}^{-1}$  region [43].

A strong absorption peak at 4796  $\text{cm}^{-1}$  can be observed in the final absorption peak region. This peak is associated with the combination of main hydroxyl stretching and Al-OH bending modes. Similar results have been reported in previous studies [11,41]. The IR absorption spectrum can mainly divide in to six regions as depicted in Figure 6. The demarcated regions of 1000 to 2050, 2300 to 3000, 3000 to 3780, 3780 to 4100, 4200 to 4850, and 6000 to 7000  $\text{cm}^{-1}$  can correspond to stretching of Al-O and Si-O, stretching of topaz-OH and OD, stretching of crystallographically bound OH and defect OH, mirror image of 3300  $\text{cm}^{-1}$  to 3500  $\text{cm}^{-1}$  absorptions, stretching of OH and bending of Al-OH, and optical transition of  $\text{Co}^{2+}$  ions respectively (Figure 6).

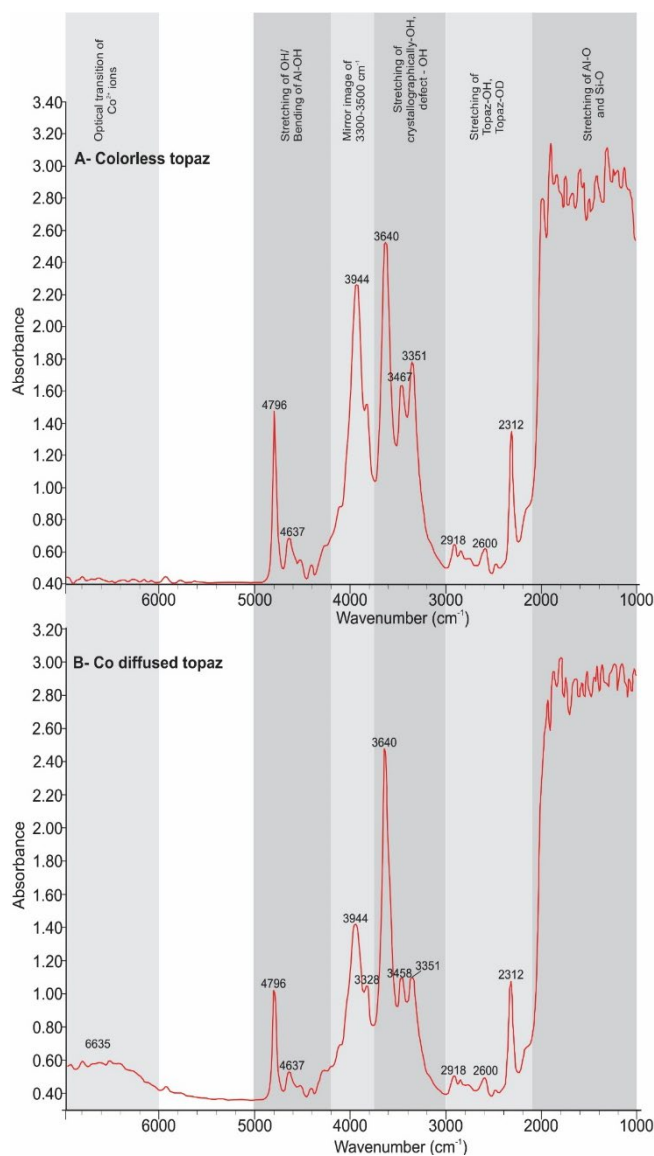
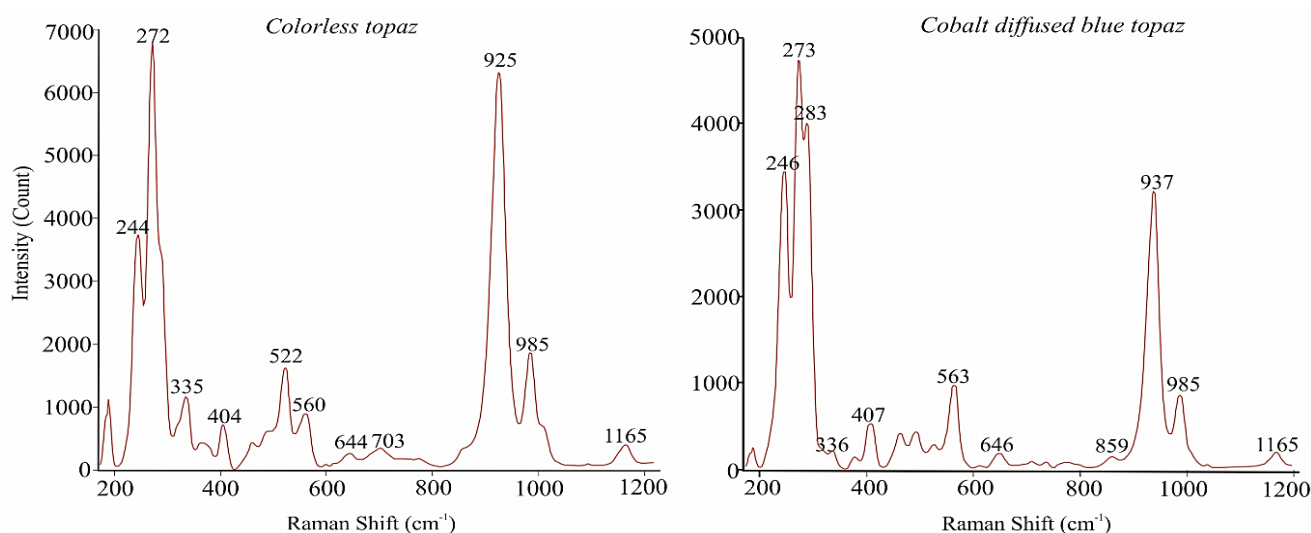


Figure 6. Infrared absorption spectrum of cobalt diffused and natural topaz.



**Figure 7.** Raman spectrum of colorless topaz and cobalt diffused blue topaz.

There are two distinguished features of IR absorption spectra observed between Co diffused topaz and colorless topaz. In case of Co diffused topaz, one additional new broader IR absorption peak has been noticed around 6640  $\text{cm}^{-1}$ . On the contrary, colorless topaz does not show any absorption around 6640  $\text{cm}^{-1}$ . Previous studies on Co doped or bearing minerals (quartz, spinel and staurolite) have given IR absorption peaks at 5350  $\text{cm}^{-1}$  to 8250  $\text{cm}^{-1}$  due to optical transitions of  ${}^4A_2 \rightarrow {}^4T_1$  in  $\text{Co}^{2+}$  ( ${}^4F$ ) [28-30]. Among them, one of the absorption peaks at 6640  $\text{cm}^{-1}$  has appeared in Co bearing blue spinel. Therefore, presumably this broad peak reported in the Co diffused topaz may assigned to Co ions. Depth profile investigations of Co diffused blue topaz using X-ray Photoelectron Spectroscopy (XPS) have revealed that Co concentrate near the surface  $\sim 4$  (at%) and it reached its maximum 8 (at%) at around 50 nm. Then, from the depth of  $\sim 80$  nm to  $\sim 200$  nm, Co concentration gets decreased exponentially [5] (please see the supplementary Figure S1). The results imply that Co atoms are concentrated within the outer surface layer and are a prerequisite for blue coloration. Subsequently, the IR peak of 6640  $\text{cm}^{-1}$  presumably corresponds due to optical transitions of  ${}^4A_2 \rightarrow {}^4T_1$  in  $\text{Co}^{2+}$  of this outer layer. Other contradictory feature of Co diffused topaz is slightly low intensity of peaks at 3351  $\text{cm}^{-1}$  and 3453  $\text{cm}^{-1}$  than colorless topaz. Past research have emphasized that, peak intensity associated with OH groups attached to the lattice defects of the topaz was decreased with temperature [35,43]. Therefore, this newly obtained IR absorption data have clearly shown that “defective” hydroxyl content has reduced with temperature that has been applied in the cobalt diffusion process.

Raman spectroscopic analysis resulted similar spectra for both natural colorless and cobalt diffused blue topaz treated at 900°C and 950°C. In the spectrums, several Raman shifts were clearly visible. In colorless topaz, the shifts were appeared at 244, 272, 335, 404, 522, 560, 644, 703, 925, 985, and 1165  $\text{cm}^{-1}$  levels (Figure 7(a)) while in Co diffused topaz they were at 246, 273, 283, 336, 407, 563, 646, 859, 937, 985, and 1165  $\text{cm}^{-1}$  (Figure 7(b)). The Raman spectra of this study nearly match with those of previous studies [16,22, 35,42]. Raman peaks at 272, 644, 855, 927, 983 and 1163  $\text{cm}^{-1}$  are due to various Si-O vibrational modes of  $\text{SiO}_4$  group [16,35]. The Raman peak at 1165  $\text{cm}^{-1}$  is associated with in plane stretching modes

of hydroxyl ions [22]. In the present study, that peak was not observed at 1163  $\text{cm}^{-1}$  position, however, it has slightly shifted to 1165  $\text{cm}^{-1}$  (Figure 7). In addition, Raman peaks at 405  $\text{cm}^{-1}$  and 522  $\text{cm}^{-1}$  are assigned to the stretching and bending modes of  $\text{AlO}_6$  octahedra coupled with the bending modes of  $\text{SiO}_4$  tetrahedra. Raman peaks at 244  $\text{cm}^{-1}$  and 336  $\text{cm}^{-1}$  are given by symmetric Si-O ring deformation and stretching of Al-F bonds respectively [22].

There were two disparate features of Raman peaks observed between Co diffused blue topaz and colorless topaz. The Raman peaks intensity of Si-related bonds were comparatively low in the Co diffused blue topaz. Moreover, the Raman peak at 522  $\text{cm}^{-1}$  was disappeared in the Co diffused topaz (Figure 7). These distinctive features of the Raman spectra may attribute to the possible phase changes occur in the outermost layer of Co diffused topaz.

#### 4. Conclusions

In value addition of low quality gem stones, expose into comparatively low temperature and low soaking time is important to reduce internal damages. However, the optimum condition for Co diffusion to Sri Lankan colorless topaz is hitherto unknown. In the present study, cobalt diffusion in Sri Lankan topaz was successfully carried-out at comparatively low temperature with a short soaking period and the study revealed and introduce for the first time, that the optimum temperature is 950°C with a soaking time of 11 h.

Foremost finding of this study is the elucidation of coloration mechanism based on the resultant colors, resultant UV-Visible absorption spectra and IR absorption spectra. Moreover, blue coloration of Co diffused topaz may attributed the by spin-allowed electronic transitions of  $\text{Co}^{2+}$  ions in tetrahedral site of topaz matrix where it substitutes for  $\text{Si}^{4+}$  ions. Likewise, the green color of diffused topaz represents an unstable lattice phase of topaz where the cobalt ions occupy unfavorable lattice sites. Thus, this newly interpreted data clearly explain the color formation mechanism of Co diffused blue topaz. Finally, the present study clearly suggests that the Sri Lankan colorless topaz can be treated easily and shows a high potential to be used as a valuable blue color gem variety in the industry.

## Acknowledgements

The authors acknowledge to Mr. Vijith Kodithuwakku for sample preparation.

## References

- [1] M. V. B. Pinheiro, C. Fantini, K. Krambrock, A. I. C. Persiano, M. S. S. Dantas, and M. A. Pimenta, "OH/F substitution in topaz studied by Raman spectroscopy," *Physical Review B - Condensed Matter and Materials Physics*, vol. 65, pp. 1-6, 2002.
- [2] M. Gaft, R. Reisfeld, and G. Panczer, *Modern Luminescence Spectroscopy of Minerals and Materials*, Second Edi. Springer International Publishing Switzerland, 2015.
- [3] D. N. Da Silva, K. J. Guedes, M. V. B. Pinheiro, S. Schweizer, J. M. Spaeth, and K. Krambrock, "The O- (Al<sub>2</sub>) centre in topaz and its relation to the blue colour," *Physica Status Solidi C: Conferences*, vol. 2, pp. 397-400, 2005.
- [4] K. Boonsook, W. Kaewwiset, P. Limsuwan, and K. Naemchanthara, "Gamma ray evaluation of fast neutron irradiated on topaz from Sri Lanka by HPGe gamma ray spectrometry," *Journal of Physics: Conference Series*, vol. 901, 2017.
- [5] H. Gabasch, F. Klauser, E. Bertel, and T. Rauch, "Coloring of topaz by coating and diffusion processes: An X-Ray photoemission study of what happens beneath the surface," *Gems & Gemology*, vol. 44, pp. 148-154, 2008.
- [6] R. Pollak, "Method for enhancing the color of minerals useful as gemstones," 1997.
- [7] P. P. Rout, R. K. Sahoo, S. K. Singh, and B. K. Mishra, "Spectroscopic investigation and colour change of natural topaz exposed to PbO and CrO<sub>3</sub> vapour," *Vibrational Spectroscopy*, vol. 88, pp. 1-8, 2017.
- [8] K. Nssau, and B. E. Pnnscore, "Blue and brown topaz produced by gamma Irradiation," *American Mineralogist*, vol. 60, pp. 705-709, 1975.
- [9] A. R. P. L. Albuquerque, S. Isotani, and S. P. Morato, "Irradiation and heating effects in topaz crystals from minas cerais, Brazil," *Radiation Effects*, vol. 106, pp. 143-150, 1988,
- [10] K. Nassau, "Altering the color of topaz," *Gems & Gemology*, vol. 21, pp. 26-34, 1985.
- [11] A. Maneewong, K. Pangza, T. Charoennam, N. Thamrongsiripak, and N. Jangsawang, "The impact of electron beam irradiation in topaz quality enhancement," *Journal of Physics: Conference Series*, vol. 1285, pp. 1-7, 2019.
- [12] N. M. A. Mohamed, and M. A. Gaheen, "Design of fast neutron channels for topaz irradiation," *Nuclear Engineering and Design*, vol. 310, pp. 429-437, 2016.
- [13] C. E. Ashbaugh, and James E. Shigley, "Reactor-irradiated green topaz," *Gems & Gemology*, vol. 29, pp. 116-121, 1993.
- [14] E. H. Christiansen, D. M. Burt, M. F. Sheridan, and R. T. Wilson, "The petrogenesis of topaz rhyolites from the western United States," *Contributions to Mineralogy and Petrology*, vol. 83, pp. 16-30, 1983.
- [15] S. Illangasinghe, S. Wickramarathna, S. Diyabalanage, L. Herath, P. Francis, and C. Jaliya, "Gem Trader's perception on treatment of low gem quality minerals, ratnapura, sri lanka," in *International Research Conference of UWU-2019*, 2019, p. 474. Accessed: Apr. 07, 2020. [Online]. Available: <http://www.erepo.lib.uwu.ac.lk/handle/123456789/672>
- [16] V. Skvortsova, N. Mironova-Ulmane, L. Trinkler, and G. Chikvaidze, "Optical properties of natural topaz," *IOP Conference Series: Materials Science and Engineering*, vol. 49, 2013.
- [17] A. C. S. Sabioni, G. M. da Costa, J. M. Dereppe, C. Moreaux, and C. M. Ferreira, "Behaviour of Brazilian imperial topaz at high temperature," *The Journal of Gemmology*, vol. 28, pp. 283-290, 2003.
- [18] M. S. Hampar and J. Zussman, "The thermal breakdown of Topaz," *TMPM Tschermaks Mineralogische und Petrographische Mitteilungen*, vol. 33, pp. 235-252, 1984.
- [19] R. A. Day, E. R. Vance, D. J. Cassidy, and J. S. Hartman, "The topaz to mullite transformation on heating," *Journal of Materials Research*, vol. 10, pp. 2963-2969, 1995.
- [20] R. W. Hughes, and T. Underwood, "Surface enhanced topaz," *Journal of the Accredited Gemologist Association*, vol. Winter, pp. 1-8, 1999.
- [21] F. Colombo, R. Lira, and E. V. Pannunzio Miner, "Mineralogical characterization of topaz from miarolitic pegmatites and w-bearing greisen in the a-type el portezuelo granite, papachacra (Catamarca Province)," *Revista de la Asociación Geológica Argentina*, vol. 64, pp. 193199, 2009.
- [22] T. Gauzzi, L. M. Graça, L. Lagoeiro, I. de Castro Mendes, and G. N. Queiroga, "The fingerprint of imperial topaz from Ouro Preto region (Minas Gerais state, Brazil) based on cathodoluminescence properties and composition," *Mineralogical Magazine*, vol. 82, pp. 943-960, 2018.
- [23] P. P. Rout, R. K. Sahoo, S. K. Singh, and B. K. Mishra, "Spectroscopic investigation and colour change of natural topaz exposed to PbO and CrO<sub>3</sub> vapour," *Vibrational Spectroscopy*, vol. 88, pp. 1-8, 2017.
- [24] G. D. Gatta, F. Nestola, G. D. Bromiley, and S. Loose, "New insight into crystal chemistry of topaz: A multi-methodological study," *American Mineralogist*, vol. 91, p. 1839ñ1846, 2006.
- [25] A. Agangi, A. Gucsik, H. Nishido, K. Ninagawa, and V. S. Kamenetsky, "Relation between cathodoluminescence and trace-element distribution of magmatic topaz from the Ary-Bulak massif, Russia," *Mineralogical Magazine*, vol. 80, pp. 881-899, 2016.
- [26] G. Lehmann, "Interstitial incorporation of di- and trivalent cobalt in quartz," *Journal of Physics and Chemistry of Solids*, vol. 30, pp. 395-399, 1969.
- [27] V. D'Ippolito, G. B. Andreozzi, U. Hålenius, H. Skogby, K. Hametner, and D. Günther, "Color mechanisms in spinel: cobalt and iron interplay for the blue color," *Physics and Chemistry of Minerals*, vol. 42, pp. 431-439, 2015.
- [28] L. C. B. d. M. Pinto, A. Righi, F. S. Lameiras, F. G. S. da Araujo, and K. Krambrock, "Origin of the color in cobalt-doped quartz," *Physics and Chemistry of Minerals*, vol. 38, pp. 623-629, 2011.
- [29] M. N. Taran, M. Koch-Müller, and A. Feenstra, "Optical spectroscopic study of tetrahedrally coordinated Co<sup>2+</sup> in natural spinel and staurolite at different temperatures and pressures," *American Mineralogist*, vol. 94, pp. 1647-1652, 2009.

- [30] P. J. Dereń, W. Stręk, U. Oetliker, and H. U. Güdel, "Spectroscopic properties of  $\text{Co}^{2+}$  ions in  $\text{MgAl}_2\text{O}_4$  spinels," *physica status solidi (b)*, vol. 182, pp. 241-251, 1994.
- [31] B. Chauviré, B. Rondeau, E. Fritsch, P. Ressaygeac, and J.-L. Devidal, "Blue spinel from the luc yen district of Vietnam | gems & Gemology," *Gems & Gemology*, vol. 51, 2015.
- [32] J. Popović, E. Tkalčec, B. Gržeta, and B. Rakvin, "Inverse spinel structure of Co-doped gahnite," *American Mineralogist*, vol. 94, pp. 771-776, 2009.
- [33] R. G. Burns, *Mineralogical applications of crystal field theory. Second edition*. Cambridge University Press; Cambridge Topics in Mineral Physics and Chemistry, 5, 1993.
- [34] P. J. Alonso, and R. Alcalá, "On the optical absorption spectrum of  $\text{Co}^{2+}$  in  $\text{CaF}_2$ ," *Physica Status Solidi (b)*, vol. 81, pp. 333-339, 1977.
- [35] D. N. Souza, J. F. de Lima, M. E. G. Valerio, C. Fantini, M. A. Pimenta, R. L. Moreira, and L. V. E. Caldas, "Influence of thermal treatment on the Raman, infrared and TL responses of natural topaz," *Nuclear Instruments and Methods in Physics Research, Section B*, vol. 191, pp. 230-235, 2002.
- [36] C. P. Smith, "A contribution to understanding the infrared spectra of rubies from Mong Hsu, Myanmar," *The Journal of Gemmology*, vol. 24, pp. 321-335, 1995.
- [37] S. V. Churakov, and A. B. Wunder, "Ab-initio calculations of the proton location in topaz-OH,  $\text{Al}_2\text{SiO}_4(\text{OH})_2$ ," *Physics and Chemistry of Minerals*, vol. 31, pp. 131-141, 2004.
- [38] C. Paikaew, J. Inthanont, A. Punyanut, E. Hoonivathana, P. Limsuwan, and K. Naemchanthara, "Effects of electron beam on structure and physical properties of natural colorless topaz," *Advanced Materials Research*, vol. 1125, pp. 60-63, 2015.
- [39] K. Komatsu, H. Kagi, T. Okada, T. Kuribayashi, J. B. Parise, and Y. Kudoh, "Pressure dependence of the OH-stretching mode in F-rich natural topaz and topaz-OH," *American Mineralogist*, vol. 90, pp. 266-270, 2005.
- [40] C. A. Londos, A. Vassilikou-Dova, G. Georgiou, and L. Fytros, "Infrared studies of natural topaz," *Physica Status Solidi (a)*, vol. 133, pp. 473-479, 1992.
- [41] P. S. R. Prasad, and T. N. Gowd, "FTIR spectroscopic study of hydroxyl ions in natural topaz," *Journal of the Geological Society of India*, vol. 61, pp. 202-208, 2003.
- [42] J. M. Beny, and B. Piriou, "Vibrational spectra of single-crystal topaz," *Physics and Chemistry of Minerals*, vol. 15, pp. 148-159, 1987.
- [43] R. D. Aines, and G. R. Rossman, "Relationships between radiation damage and trace water in zircon, quartz, and topaz," *American Mineralogist*, vol. 71, pp. 1186-1193, 1986.
- [44] A. Watenphul, and B. Wunder, "Temperature dependence of the OH-stretching frequencies in topaz-OH," *Physics and Chemistry of Minerals*, vol. 37, pp. 65-72, 2010.